CHIN. PHYS. LETT. Vol. 34, No. 4 (2017) 046601

Simulation Study on the Controllable Dielectrophoresis Parameters of Graphene *

Jian-Long Ji(冀健龙)[1,2], Ya-Li Liu(刘亚丽)[1], Yang Ge(葛阳)[1], Sheng-Dong Xie(解胜东)[1], Xi Zhang(张希)[1], Sheng-Bo Sang(桑胜波)[1**], Ao-Qun Jian(菅傲群)[1], Qian-Qian Duan(段倩倩)[1], Qiang Zhang(张强)[1], Wen-Dong Zhang(张文栋)[1]

[1]*Key Lab of Advanced Transducers and Intelligent Control System (Ministry of Education), Taiyuan University of Technology, Taiyuan 030024*

[2]*Advanced Coal Mine Machinery and Equipment Collaborative Innovation Center of Shanxi Province, Taiyuan University of Technology, Taiyuan 030024*

(Received 19 December 2016)

The method of using dielectrophoresis (DEP) to assemble graphene between micro-electrodes has been proven to be simple and efficient. We present an optimization method for the kinetic formula of graphene DEP, and discuss the simulation of the graphene assembly process based on the finite element method. The simulated results illustrate that the accelerated motion of graphene is in agreement with the distribution of the electric field squared gradient. We also conduct research on the controllable parameters of the DEP assembly such as the alternating current (AC) frequency, the shape of micro-electrodes, and the ratio of the gap between electrodes to the characteristic/geometric length of graphene (λ). The simulations based on the Clausius–Mossotti factor reveal that both graphene velocity and direction are influenced by the AC frequency. When graphene is close to the electrodes, the shape of micro-electrodes will exert great influence on the velocity of graphene. Also, λ has a great influence on the velocity of graphene. Generally, the velocity of graphene would be greater when λ is in the range of 0.4–0.6. The study is of a theoretical guiding significance in improving the precision and efficiency of the graphene DEP assembly.

PACS: 66.20.Cy, 64.70.qj, 47.65.−d DOI: 10.1088/0256-307X/34/4/046601

In recent years, graphene-based devices have attracted considerable attention due to their excellent electronic properties.[1,2] Consequently, electronic devices such as logic circuits, field effect transistors and super capacitors have been widely investigated.[3,4] Generally, such devices can be fabricated either in a top-down approach, where graphene is first grown on a substrate and subsequently contacted by electrodes, or a bottom-up method where the electrodes are prefabricated and graphenes subsequently need to be assembled at the expected locations.[5]

In terms of top-down approach, the most popular method is cleaving bulk graphite micromechanically.[6,7] However, this suffers from a low-yield process which is unsuitable for controlled and scaled-up devices fabrication. As for the bottom-up method, graphene can be produced by chemical vapor deposition,[8,9] which is believed to be one of the most promising ways for manufactory purpose, or mechanical exfoliation in solutions.[10] Then, a directed assembly process of graphene flakes at predetermined locations is thus required.

DEP is a simple and effective method utilized to assemble graphene to the micro-electrodes.[11] For example, single-layer graphene oxide was placed between the electrodes by Burg *et al.*[12] and graphene was deposited on silicon wafers by Li *et al.*[13] The existing works generally concentrate on DEP parameters such as the process time, voltage of the electric field and the concentration of graphene to investigate the mechanism and its feasibility.[14] However, there are some other important parameters which may influence experimental efficiency and cost seriously. In this study, we concentrate more on the alternating current (AC) frequency, the shape of the micro-electrodes, and the ratio of the gap between electrodes to the graphene characteristic length.

Though various experiments of graphene dielectrophoresis have been reported in recent decades,[15] there are seldom reports on simulations of graphene trajectories to the best of our knowledge. Generally, researchers tend to calculate the electric field[16] or the gradient of the square of the electric field[17] since there are several obstacles, such as how to describe a sheet with thickness ranging from a single monolayer to several layers by continuum mechanics and how to establish the mathematical model illustrating the forces balancing in a liquid environment, which must be overcome to obtain the motion trail of graphene.

Based on the DEP theory, graphene flakes can reach a balance in a liquid environment[18] because of the DEP force and the viscous drag force. When an AC signal is applied to the electrodes, a non-uniform electric field develops which will further polarize graphene flakes and will result in a Coulomb force. Meanwhile, graphene flakes' motion is impeded by a viscous drag force owing to the mutual interactions between the flakes and the surrounding liquid. On the other hand, the mathematical model of nanotubes and nanowires DEP is widely used,[19,20] and is proved to

*Supported by the Basic Research Project of Shanxi Province under Grant No 2015021092, the National Natural Science Foundation of China under Grant Nos 61471255, 61474079, 61501316, 51505324 and 51622507, and the National High-Technology Research and Development Program of China under Grant No 2015AA042601.

**Corresponding author. Email: sangshengbo@tyut.edu.cn

© 2017 Chinese Physical Society and IOP Publishing Ltd

be efficient to describe the motion of one-dimensional nanomaterials[21] during the dielectrophoresis process through the finite element method (FEM). The DEP model is a function of object's geometries, the gradient of the square of the electric field, the conductivity and permittivity of the objects and solutions.[22] Therefore, we attempt to put carbon nanotubes together to obtain the motion path of several layers of graphene flakes through FEM (Fig. 1), because the gradient of the square of the electric field is a vector which can be added in the space while the other factors could be taken as constant even though there are numerous differences of physical and chemical properties between carbon nanotubes and graphene.

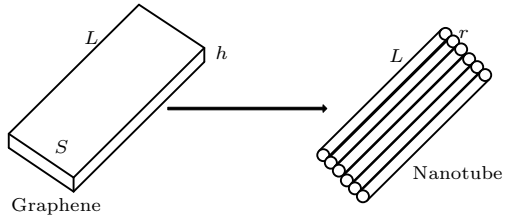

Fig. 1. Physical model of graphene flakes made up by carbon nanotubes.

The DEP force of a carbon nanotube can be expressed as[22,23]

$$F_{\mathrm{DEP1}} = \frac{\pi r^2}{6}\varepsilon_{\mathrm{m}}\mathrm{Re}[k(\omega)]\nabla E^2, \tag{1}$$

where L is the length of the carbon nanotube, r is its radius, $\mathrm{Re}[k(\omega)]$ is the real component of the Clausius–Mossotti factor $k(\omega)$, and ∇E^2 is the gradient of the electric field squared.

The Clausius–Mossotti factor is shown by

$$k(\omega) = \frac{{\varepsilon_{\mathrm{p}}}^* - {\varepsilon_{\mathrm{m}}}^*}{{\varepsilon_{\mathrm{p}}}^* + 2{\varepsilon_{\mathrm{m}}}^*}, \quad \varepsilon^* = \varepsilon - i * \frac{\sigma}{\omega}, \tag{2}$$

$$\begin{aligned}\mathrm{Re}[k(\omega)] = &\Big[(\varepsilon_{\mathrm{p}} - \varepsilon_{\mathrm{m}})(\varepsilon_{\mathrm{p}} + 2\varepsilon_{\mathrm{m}}) \\ &+ \frac{1}{\omega^2}(\sigma_{\mathrm{p}} - \sigma_{\mathrm{m}})(\sigma_{\mathrm{p}} + 2\sigma_{\mathrm{m}})\Big] \\ &\cdot\Big[(\varepsilon_{\mathrm{p}} + 2\varepsilon_{\mathrm{m}})^2 + \frac{1}{\omega^2}(\sigma_{\mathrm{p}} + 2\sigma_{\mathrm{m}})^2\Big]^{-1},\end{aligned} \tag{3}$$

where the subscripts p and m represent the carbon nanotube and the medium, respectively, ε^* is the complex permittivity, σ is the conductivity, and ω is the frequency of the external electric field.

The viscous drag force can be expressed as

$$f_1 = \frac{6\pi\eta L}{\ln\frac{2L}{r}}, \tag{4}$$

where η is the dynamic viscosity of the fluid medium.

Then, the velocity of carbon nanotube can be expressed as

$$v = \frac{F_{\mathrm{DEP1}}}{f_1}. \tag{5}$$

According to our previous discussion, DEP force, viscous drag force and velocity of graphene flakes can be expressed approximately as

$$F_{\mathrm{DEP}} = \sum_{1}^{\frac{sh}{4r^2}} \frac{1}{6}\pi L r^2 \varepsilon_{\mathrm{m}} \nabla_{E_i}{}^2 \mathrm{Re}[k(\omega)], \tag{6}$$

$$f = \frac{sh}{4r^2} f_1, \tag{7}$$

$$v = \frac{F_{\mathrm{DEP}}}{f}, \tag{8}$$

where h and s represent the thickness and the cross-sectional area perpendicular to the direction of thickness, respectively.

Based on the requirement of the assembly process and Eqs. (6)–(8), the FEM model is built in the following, which includes the graphene flakes, an ellipsoid DI water environment and two Au electrodes (Fig. 2). The parameters of materials are listed in Table 1.

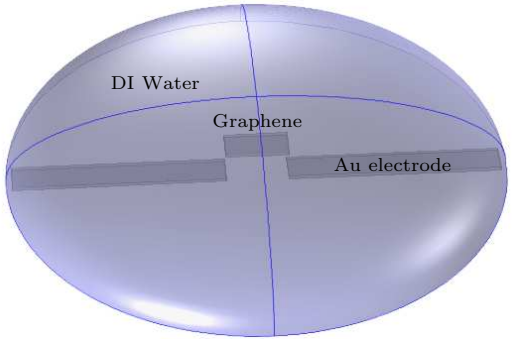

Fig. 2. The FEM model of graphene flakes in the DI water.

Table 1. Parameters of materials.

Material	Conductivity (s/m)	Relative permittivity
Graphene	30000[a]	3.5[a]
DI water	5.5×10^{-6}[b]	78.5[b]
Au electrode	10^7	1

[a]Refs. [24–26], and [b]Ref. [27].

The AC frequency not only influences the magnitude of the graphene velocity but also its direction. Equations (2) and (3) indicate that the DEP force depends on the frequency of the external electric field because of $\mathrm{Re}[k(\omega)]$. It will generate a positive DEP force, which would attract graphene towards the gap of micro-electrodes when $\mathrm{Re}[k(\omega)]$ is positive.[28] In contrast, graphene is repelled. As illustrated in Fig. 3, the influence of frequency on the accelerated motion of graphene has been demonstrated where different AC frequencies have been discussed. This inset also shows that $\mathrm{Re}[k(\omega)]$ rapidly translates from positive to negative within the interval of 10^{12}–10^{13} Hz. The crossover frequency labeled as f_0 indicates the frequency where $\mathrm{Re}[k(\omega)]$ is equal to zero and below which the graphene velocity is positive.

Moreover, Eq. (2) shows that f_0 is determined by both permittivity and conductivity of the medium and graphene. Therefore, it must be noted that though the crossover frequency illustrated here is much high

for the commercial signal-generators, it would dramatically decline to 10^5 Hz if factors like surfactant concentrations, which exerts great influences on the stabilization and the dispersion of carbon nanomaterials, could be taken into account.[29] Obviously, the experimental parameters in the actual investigations are very different and more complicated than the assumptions that we made here. Here 10^5 Hz is much easier to access than 10^{12} Hz. Thereafter, it is definitely essential to calculate the crossover frequency before performing every investigation.

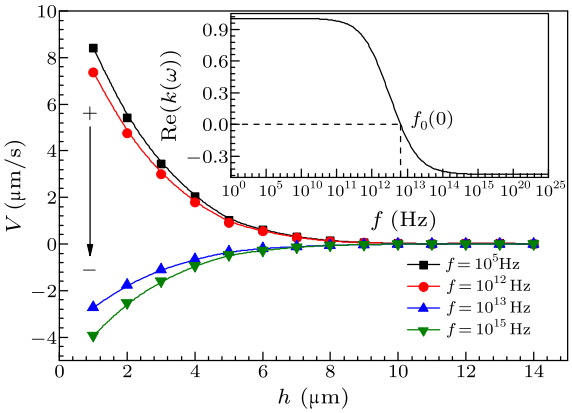

Fig. 3. Velocities of graphene versus altitude at different frequencies. The inset shows the real part of the Clausius–Mossotti factor Re[$k(\omega)$] versus the frequencies.

The shapes of micro-electrodes such as rectangular, triangular, and round are also considered. The results show that it greatly influences the velocities of graphene in the near region of micro-electrodes. Figure 4 demonstrates that when the graphene heights are lower than 6 μm, the graphene velocities produced by DEP using a rectangular or round micro-electrode are 3–8 times greater than that using the triangular micro-electrode. This agrees well with the investigation of Kwon *et al.*[30] However, there are no obvious influences when the graphene height is larger than 6 μm. In short, the shape of micro-electrodes is a significant factor affecting the efficiency of DEP assembly in the near region of micro-electrodes.

According to Eq. (6), the DEP force is proportional to ∇E^2. The inset of Fig. 4 also shows the curves of ∇E^2 varying with the graphene altitude, and there is a similar trend with velocity curves when different micro-electrode shapes are employed. For rectangular and round micro-electrodes, ∇E^2 are over 10^{17} V^2/m^3 and 10^{14} V^2/m^3 when the heights of graphene are 1 μm and 14 μm, respectively. Consequently, the graphene velocity at 1 μm height is 1000 times greater than that at 14 μm height. Hence, the results illustrate that increasing the concentration of graphene dispersed in the near region of the electrodes can improve the efficiency substantially.

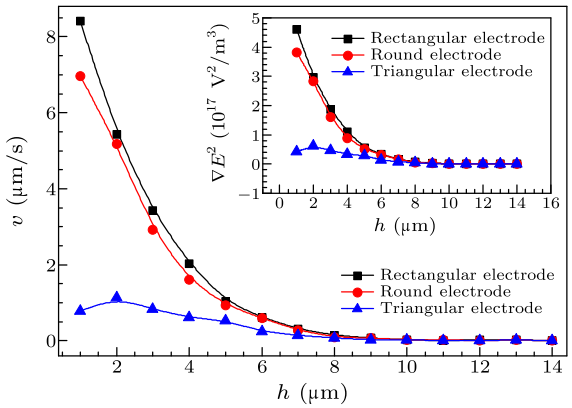

Fig. 4. Graphene velocities versus altitude with different electrode shapes. The inset shows ∇E^2 of three types of electrodes varying with the altitude.

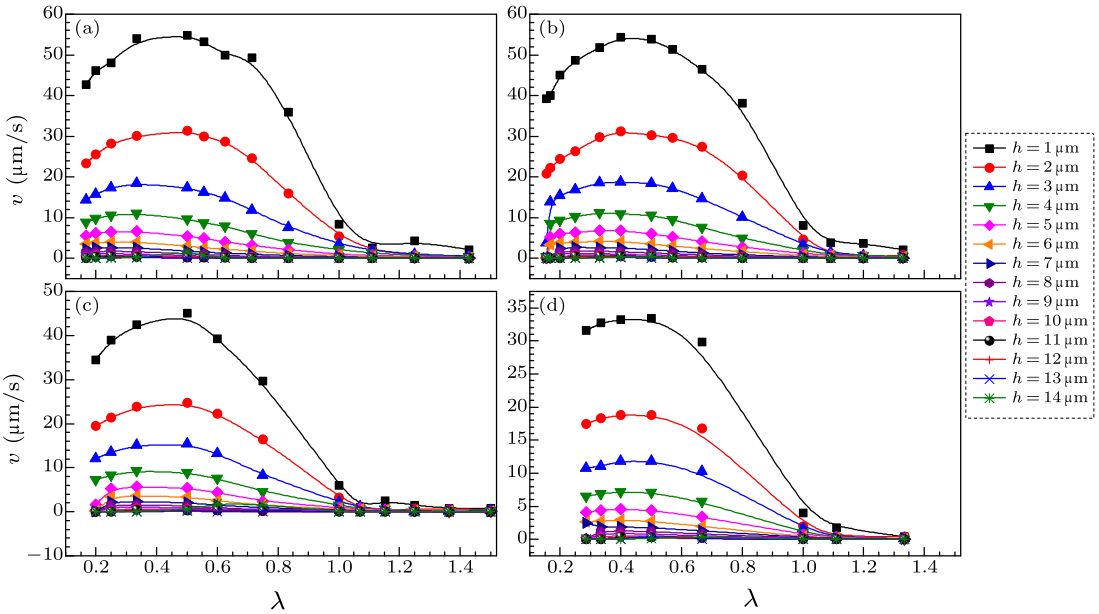

Fig. 5. Velocities of graphene influenced by λ. The gaps of two electrodes in (a)–(d) are 10 μm, 12 μm, 15 μm and 20 μm, respectively.

Technically, electron beam lithography is needed when the gap between electrodes is less than 2 μm. Therefore, the gap between electrodes is a significant factor which could increase experimental cost dramatically. To make a thorough inquiry into the influence of the gap between electrodes on the DEP assembly, λ is defined as the ratio of the gap between electrodes to the length of graphene. We obtain that the velocities of graphene are much greater when λ is in the range of 0.4–0.6.

As illustrated in Fig. 5, the velocities of graphene at different heights vary with λ where the gaps of the two electrodes are fixed at 10 μm (Fig. 5(a)), 12 μm (Fig. 5(b)), 15 μm (Fig. 5(c)) and 20 μm (Fig. 5(d)), respectively. Firstly, velocities decrease with the height of graphene, and this agrees well with the above discussions. Further, graphene velocities fluctuate with the increase of λ and reach the peak when λ is in the range of 0.4–0.6 generally. Moreover, graphene which is closer to the electrodes experiences a more intensive change of velocity. For example, Fig. 5(c) shows that when graphene is 3 μm in height, the velocity would decrease to about 1/38th when λ increases from 0.5 to 1. This illustrates that, in the x–y plane, once the length of graphene becomes shorter than twice the gap of the micro-electrodes, ∇E^2 decreases sharply. Then, the DEP force and velocity also decrease dramatically.

According to the influences law of λ, DEP assembly efficiency and precision could be improved considerably by controlling the ratio of the gap between the micro-electrodes to the length of graphene. On the other hand, it is unwise to pursue the a smaller gap though the assembly velocity is greater when λ is smaller. At present, it is very expensive to keep the electrodes' spacing to be smaller than 2 μm. Therefore, it is more reasonable and cost-effective to select graphene samples whose characteristic length is longer than 4 μm.

In summary, we have derived the mathematical model of graphene DEP from CNT DEP. Then we have built a three-dimensional model to simulate the graphene DEP process based on the FEM. The results indicate that graphene will move towards the gap of electrodes only if the frequencies of the external electric field are lower than f_0 which is decided by both permittivity and conductivity of the medium and graphene. Moreover, by comparing three different electrode geometries we have demonstrated that round and rectangular electrodes could be more efficient regarding the assembly efficiency than the triangular electrode. We also further investigate the influence of λ and report the optimal interval of λ to be 0.4–0.5. However, there are some limitations that are ignored. For example, the real surface of graphene is non-smooth and there are various kinds of shape of graphene in use. Moreover, the impacts of the overlap and deformation of graphene flakes are needed to lucubrate in further.

References

[1] Fuh Y K, Kuo C C, Huang Z M, Li S C and Liu E R 2016 *Small* **12** 1875
[2] Yan Q, Zhang S, Long X, Luo H, Wu F, Fang L, Wei D and Liao M 2016 *Chin. Phys. Lett.* **33** 078501
[3] Pei S, Zhao J, Du J, Ren W and Cheng H M 2010 *Carbon* **48** 4466
[4] Zhou X, Chen J, Gu L and Miao L 2015 *Chin. Phys. Lett.* **32** 026102
[5] Ji J J, Zhou Z Y, Yang X, Zhang W D, Sang S B and Li P W 2013 *Small* **9** 3014
[6] Zhao B, Chen T, Pan H and Mao P 2015 *Eur. Phys. J. Appl. Phys.* **72** 20401
[7] Zhang H Y and Dong S L 2013 *Chin. Phys. Lett.* **30** 043102
[8] Zhang L, Shi Z, Yang R and Huang J 2014 *Chin. Phys. Lett.* **31** 097301
[9] Yuan G D, Zhang W J, Yang Y, Tang Y B, Li Y Q, Wang J X, Menget X M, He Z B, Wu C M L, Bello I, Lee C S and Lee S T 2009 *Chem. Phys. Lett.* **467** 361
[10] Liang F, Watanabe T, Hayashi K, Yao Y, Ma W, Yang B and Dai Y 2017 *Mater. Lett.* **187** 32
[11] Singh B, Wang J, Rathi S and Kim G H 2015 *Appl. Phys. Lett.* **106** 103103
[12] Burg B R, Schneider J, Maurer S, Schirmer N C and Poulikakos D 2010 *J. Appl. Phys.* **107** 034302
[13] Li P, Lei N, Xu J and Xue W 2012 *IEEE Trans. Nanotechnol.* **11** 751
[14] Oikonomou A, Clark N, Heeg S, Kretinin A, Varey S, Yu G L and Vijayaraghavan A 2015 *Phys. Status Solidi RRL (RRL)-Rapid Res. Lett.* **9** 539
[15] Macnaughton S, Ammu S, Manohar S K and Sonkusale S 2014 *PLoS ONE* **9** e111377
[16] Wang J, Singh B, Park J H, Rathi S, Lee I Y, Maeng S, Joh H I, Lee C H and Kim G H 2014 *Sens. Actuators* B **194** 296
[17] Peng Y and Lei J 2014 *Nanoscale Res. Lett.* **9** 617
[18] Lei U and Lo Y J 2011 *Iet Nanobiotechnology* **5** 86
[19] Liu Y, Chung J H, Liu W K and Ruoff R S 2006 *J. Phys. Chem.* B **110** 14098
[20] Montemurro D, Stornaiuolo D, Massarotti D, Ercolani D, Sorba L, Beltram F, Tafuri F and Roddaro S 2015 *Nanotechnology* **26** 385302
[21] An L and Friedrich C R 2009 *J. Appl. Phys.* **105** 074314
[22] Smith B D, Mayer T S and Keating C D 2012 *Annu. Rev. Phys. Chem.* **63** 241
[23] Berger S D, Mcgruer N E and Adams G G 2015 *Nanotechnology* **26** 155602
[24] ChavezValdez A, Shaffer M S and Boccaccini A R 2013 *J. Phys. Chem.* B **117** 1502
[25] Huang X, Qi X, Boey F and Zhang H 2012 *Chem. Soc. Rev.* **41** 666
[26] Wang J W, Singh B, Maeng S, Joh H I and Kim G H 2013 *Appl. Phys. Lett.* **103** 083112
[27] Wang Y, Du F, Pesch G R, Köser J, Baune M and Thöming J 2016 *Chem. Eng. Sci.* **153** 34
[28] Yang L 2012 *Anal. Lett.* **45** 187
[29] Hennrich F, Krupke R, Kappes M M and Löhneysen H V 2005 *J. Nanoscience Nanotechnol.* **5** 1166
[30] Kwon S H, Jeong Y K, Kwon S, Kang M C and Lee H W 2011 *Trans. Nonferrous Met. Soc. Chin.* **21** S126